

Large-Scale Nanoelectrode Arrays to Monitor the Dopaminergic Differentiation of Human Neural Stem Cells

Tae-Hyung Kim, Cheol-Heon Yea, Sy-Tsong Dean Chueng, Perry To-Tien Yin, Brian Conley, Kholud Dardir, Yusin Pak, Gun Young Jung, Jeong-Woo Choi,* and Ki-Bum Lee*

Over the last decade, stem-cell-based therapy has emerged as a promising therapeutic strategy with significant implications for regenerative medicine due to the intrinsic ability of stem cells to differentiate into practically any given cell type.^[1] For instance, human neural stem cells (hNSCs) are multipotent and have the ability to differentiate into both neurons and glial cells (e.g., oligodendrocytes, astrocytes, and microglia).^[2] As such, they hold immense potential for the treatment of neurological diseases/disorders such as Alzheimer's disease, Parkinson's disease (PD), Huntington's disease, and spinal cord injury.^[3] In the case of PD, stem-cell-based research has typically focused on the transplantation of stem-cell-derived dopaminergic neurons as PD is primarily caused by the loss of dopaminergic neurons in the substantia nigra of the mid brain.^[4] To identify and characterize these differentiated cells, which is critical to achieve prior to transplantation, fluorescence-based methods (e.g., immunostaining and FACS) and biomolecular analysis of the expression of biomarkers (DNAs/RNAs/proteins) are currently widely used. These techniques are highly sensitive and, as a result, can be used to precisely determine the biological characteristics of differentiated cells; however, they tend to be laborious, time-consuming, and most importantly, involve destructive steps such as cell fixation or cell lysis, which prevents the subsequent use of these characterized cells for clinical applications. As such, to realize the full potential of stem-cell-based therapies, there is an urgent need for techniques that can not only effectively identify stem cell fate but also do so in non-destructive and quantitative manner.

Addressing these challenges, we report a novel cell-based sensing platform (large-scale homogeneous nanocup-electrode arrays (LHONA)) that is capable of achieving real-time and highly sensitive electrochemical detection of neurotransmitters that are produced from dopaminergic cells. As such, it can discriminate dopaminergic neurons from other types of cells in a completely noninvasive and label-free manner (Figure 1). In particular, LHONA is composed of distinct periodic cup-like nanostructures that were generated on an indium tin oxide (ITO) electrode (1.5 cm × 1.5 cm) via sequential laser interference lithography (LIL) and electrochemical deposition (ECD) methods. Owing to its unique nanoscale structure, LHONA has a number of advantages over other cell-based biosensors. First, recent studies have reported that nanostructured arrays can enhance cell functions via the spatiotemporal and dynamic rearrangement of focal adhesions and the cellular cytoskeleton.^[5] As such, LHONA overcomes one of the major challenges faced by current cell-based biosensors, specifically their dependence on cell adhesive molecules to promote cell anchoring to the electrode, which can adversely decrease the achievable sensitivity.^[6] On the other hand, the 3D nanostructures of LHONA are also highly preferred for detecting electrochemical signals owing to their capability to improve the selectivity, sensitivity, and spatial resolution. Hence, by combining these aforementioned advantages, we demonstrated that LHONA can serve as an outstanding platform for the sensitive detection of both dopamine (DA) exocytosed from a model dopaminergic cell line (PC12) and dopaminergic neurons derived from hNSCs via the direct attachment/culturing of cells on the surface of LHONA in a biocompatible and nondestructive manner (Figure 1a). This enabled the sensitive discrimination of dopamine-producing neurons from other cell types including progenitor cells (hNSCs, neurospheres, and premature neurons), nondopaminergic neurons, and other cell types (astrocytes and human dermal fibroblasts) (Figure 1b).

Figure 2a illustrates the experimental steps that were used to obtain the periodic metal nanostructures. Briefly, homogeneous photoresist (PR) grid nanopatterns were first fabricated on the surface of ITO using LIL with different sizes and shapes (Figure 2b, Figure S1 in the Supporting Information). Thereafter, the PR nanoholes were utilized as a template to deposit gold using the ECD method. By carefully adjusting the solution composition (e.g., concentration of gold chloride and type of surfactant) and the electrochemical parameters (e.g., voltage applied and time), which are related to the growth rate parallel or perpendicular to the direction of the current,^[7] distinct cup-like or dot-like nanostructures were successfully generated on the entire ITO electrode (Figure 2b, Figure S2b in the

Dr. T.-H. Kim, Dr. C.-H. Yea, S.-T. D. Chueng,
B. Conley, K. Dardir, Prof. K.-B. Lee
Department of Chemistry and Chemical Biology
Rutgers, The State University of New Jersey
Piscataway, NJ 08854, USA
E-mail: kblee@rutgers.edu

Dr. C.-H. Yea, Prof. J.-W. Choi
Department of Chemical & Biomolecular Engineering
Sogang University
Seoul 121-742, Republic of Korea
E-mail: jwchoi@sogang.ac.kr

P. T.-T. Yin, Prof. K.-B. Lee
Department of Biomedical Engineering
Rutgers, The State University of New Jersey
Piscataway, NJ 08854, USA

Y. Pak, Prof. G. Y. Jung
School of Materials Science and Engineering
Gwangju Institute of Science and Technology (GIST)
Gwangju 500-712, Republic of Korea



DOI: 10.1002/adma.201502489

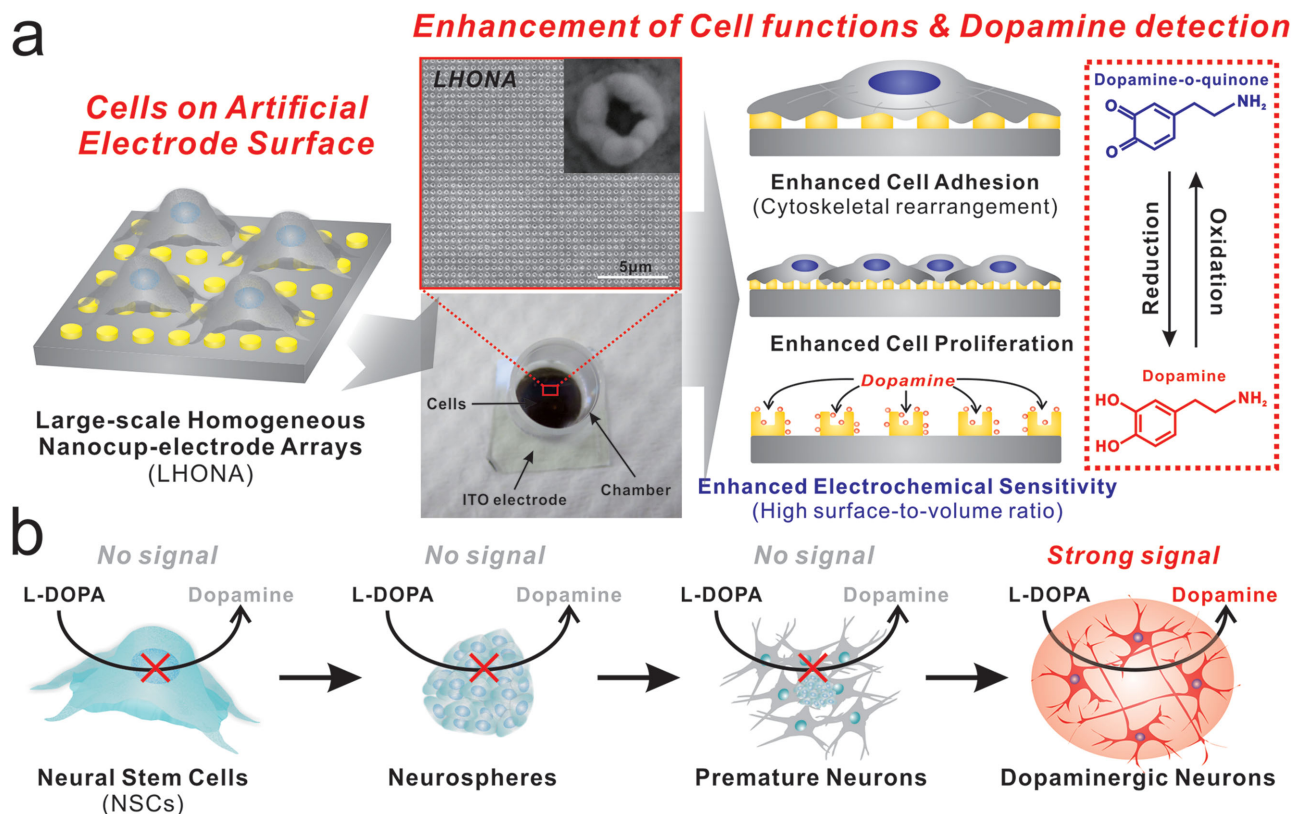


Figure 1. a) Schematic diagram representing superiority of large-scale homogeneous nanocup electrode arrays (LHONA) as a conductive cell culture platform which enhances major cell functions, as well as electrochemical sensitivity toward dopamine detection, both are extremely important for cell-based sensors. Picture is a cell-based chip used for the detection of dopamine released from dopaminergic cells that is composed of ITO electrode, LHONA, and the chamber for cell culture. Image above is the structure of LHONA characterized by scanning electron microscopy. b) Detection strategy for the discrimination of dopaminergic neurons from other types of their progenitor cells using L-DOPA pretreatment and LHONA as the cell culture platform (working electrode) based on electrochemical method. Only cells capable of converting L-DOPA to dopamine can give distinct redox peaks which could be used as an indicator of the presence of dopaminergic neurons.

Supporting Information). Besides the concentration of gold ions, deposition time was also a key parameter in controlling the geometry of the nanotopographic features. Patterns were formed as a thin-film-like structure within a short period of time ($t = 60$ s, Figure 2b) and finally, cup-like structures were generated when deposition time reached 240 s, which was the best platform in terms of both its topographical characteristic (Figure 2b) and its electrochemical sensitivity toward DA detection (Figure S3, Supporting Information).

Next, we compared the electrochemical performance of LHONA with other types of electrodes that use ITO as a supporting substrate in terms of sensitivity toward DA detection. As an initial proof-of-concept, we used a cell-free configuration where DA was detected in situ. At a concentration of 10×10^{-6} M DA, the cathodic peak current (I_{pc}) were not detectable on bare ITO electrodes and ITO modified with 10 nm AuNPs (gold nanoparticles), while ITO-50 nm AuNPs showed a very weak reduction peak ($I_{pc} = 0.155 \mu\text{A}$). On the other hand, ITO modified with reduced graphene oxide (rGO), which has previously been reported as an outstanding material for the detection of DA,^[8] showed better performance ($I_{pc} = 0.592 \mu\text{A}$). However, interestingly, LHONA substrates exhibited the most distinct redox peaks ($I_{pc} = 2.25 \mu\text{A}$), which was 13.5 and 2.8 times higher

than ITO-50 nm AuNPs and ITO-rGO substrates (Figure 2c, Figure S4a in the Supporting Information). Remarkably, the reduction current of LHONA (nanocups) was even higher (59.6%) than homogeneous nanoelectrode arrays [NEAs (dot-like structure)] (Figure S2b, ii, Supporting Information) generated using the same ECD method ($I_{pc} = 1.41 \mu\text{A}$), which is speculated to be due in part to the increased surface area, proving its excellent sensitivity for the electrochemical detection of DA. The redox peaks were constant and increased with increasing scan rates (20, 40, 60, 80, and 100 mV s^{-1}), proving that the cathodic peaks originated from DA and not from noise or other contaminants (Figure S5a,b, Supporting Information). Moreover, LHONA showed good linearity at both low ($0.3\text{--}3 \times 10^{-6}$ M, $R^2 = 0.99$) and high concentrations ($0\text{--}50 \times 10^{-6}$ M, $R^2 = 0.986$) of DA, with a limit of detection (LOD) of 100×10^{-9} M (Figure 2d, and Figures S4b and S5c,d in the Supporting Information). Since the fabricated substrate (LHONA) showed excellent performance in terms of DA detection, which is superior to other transparent electrodes (GNP and rGO-modified ITOs, homogeneous gold nanodot arrays), it is highly likely that LHONA will be the suitable material for effective in situ electrochemical detection of DA synthesized from dopaminergic cells in sensitive and noninvasive manner, which is at the ultimate goal of this study.

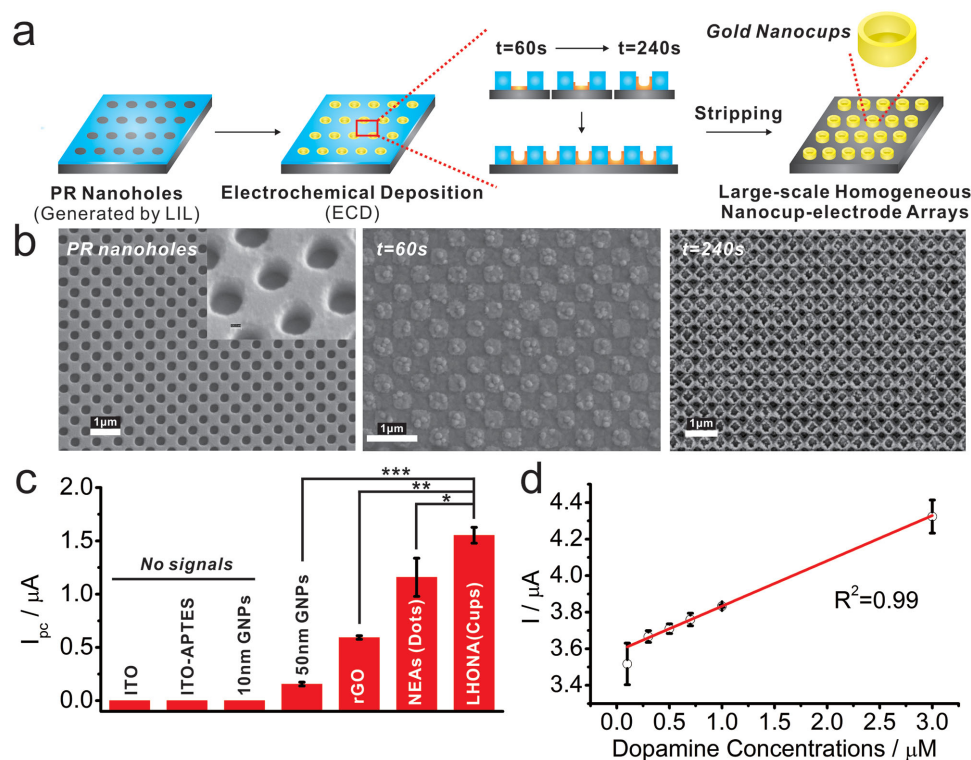


Figure 2. a) Schematic diagram showing sequential steps to generate LHONA on ITO electrode via laser interference lithography (LIL) and electrochemical deposition method. b) SEM images of (i) polymer nanohole template generated by LIL and electrochemically deposited gold nanostructures with different deposition time. c) Intensities of cathodic peaks of dopamine obtained from cyclic voltammetry using different types of substrates and (Student's *t*-test, $N = 3$, $*p < 0.05$, $**p < 0.01$, $***p < 0.001$). d) The linear correlations between concentrations of dopamine and signal intensities at reduction potential of cyclic voltammetry.

It is important to note that unlike typical biosensors, the electrode of cell-based biosensors must be highly biocompatible in order to promote cell attachment, growth, and subsequent secretion of the biomolecule of interest, which in this case is DA.^[6a,9] As such, we next investigated whether LHONA could act as an effective substrate for culturing neural cells. In particular, it was our hypothesis that the nanoscale topographic characteristics of LHONA (periodic and homogeneous) would contribute to the enhancement of cell adhesion, spreading, and growth of the model dopaminergic cells (PC12) (Figure 3a).^[5a,b,10] Since PC12 cells are highly sensitive to the adhesion materials, as expected, cell spreading on bare gold and normal tissue culture plates (TCPs) was found to be highly restricted (Figure 3b). In contrast, interestingly, PC12 cells spread well on bare LHONA [without extracellular matrix materials], where they exhibited a well-spread morphology throughout the entire surface that was similar to the cells on Matrigel-coated TCPs (Figure 3b, Figure S6 in the Supporting Information). Remarkably, the total surface area of the cells spread on the LHONA was found to be 12.4% and 88.9% higher than that on TCPs and bare gold substrates (Figure 3c, Figure S7 in the Supporting Information), respectively, and the number of cells remaining on the LHONA after washing was 270% higher than both TCP and bare gold substrates due to the enhanced cell adhesion (Figure 3d, Figure S7 in the Supporting Information). Moreover, cell proliferation was found to be increased on LHONA substrate compared to bare gold

substrates (Figure S8, Supporting Information), proving that LHONA is an excellent platform for culturing and enhancing major functions of model dopaminergic neurons which will be suitable for electrochemical study over other types of substrates. These effects of nanostructured arrays on the cell functions became completely negligible after the modification of thick Matrigel layer on LHONA, proving that the enhancement of cell functions solely originated from the distinct nanotopographical features of LHONA (Figure S9, Supporting Information).

After confirming the superior characteristics of the LHONA in terms of biocompatibility, cyclic voltammetry (CV) was applied to detect DA released from PC12 cells attached to electrode. For this purpose, L-DOPA, a precursor which can be converted to DA by DOPA decarboxylase (DDC), was added prior to the detection of DA to increase the amount of DA synthesized by the dopaminergic PC12 cells.^[6a,9] As expected, bare gold electrodes showed no redox signals regardless of treatment with L-DOPA (Figure 3e). This was hypothesized to be mainly due to the limited number of cells attached to the bare gold substrate, cell aggregation (less spreading), and limited growth, all of which indicated that the major functions of the PC12 cells were highly compromised (Figure 3b–d, Figure S6–S8 in the Supporting Information). After modification with Matrigel, the morphology of the cells and their growth were significantly improved (Figure S9, Supporting Information); however, no reduction and oxidation peaks appeared on the voltammogram owing to Matrigel blocking electron transfer to the surface of

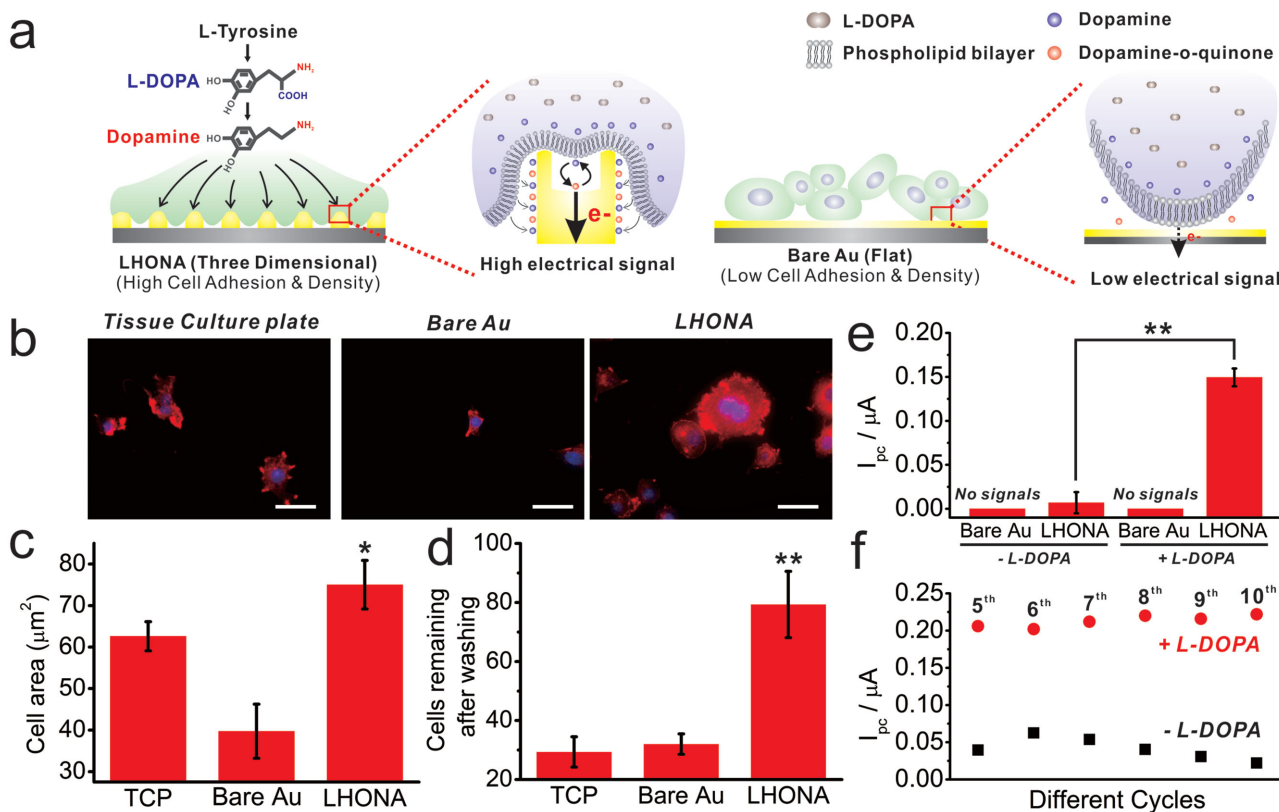


Figure 3. a) Schematic diagram showing the interaction between cell membrane and the surface of electrodes that results in the increase of electrical signals of model dopaminergic cells on LHONA due to the enhanced cell spreading, adhesion, and proliferation compared to flat (2D) surface. b) F-actin-stained fluorescence images of PC12 cells (scale bar = 40 μm), c) analysis of cell surface area (cell spreading), and d) cells remaining on the surface after washing for cell fixation which were calculated from F-actin-stained images of PC12 cells on three different substrates (Student's *t*-test, $N = 3$, $*p < 0.05$, $**p < 0.01$). e) I_{pc} values of cyclic voltammogram achieved from PC12 cells on bare Au and LHONA substrates. PC12 cells treated with L-DOPA prior to the electrochemical analysis indicated as "+L-DOPA" while cells without L-DOPA indicated as "-L-DOPA". f) I_{pc} values calculated from cyclic voltammetric curves with different cycle numbers, which were obtained from PC12 cells on LHONA-M.

the electrode. We next attempted to use a reduced amount of Matrigel (four times more diluted than normal concentration) to enhance the electron transfer from cells to the electrode; however, the diluted Matrigel modified on the gold substrate was found to be insufficient to improve cell spreading and proliferation. In contrast, interestingly, cells on LHONA showed clear reduction and oxidation peaks at -33 and 125 mV, respectively, proving its outstanding potential to be applied for in situ monitoring of DA released from dopaminergic cells (Figure 3e, Figure S10 in the Supporting Information). Remarkably, PC12 cells on diluted Matrigel-modified LHONA (LHONA-M) also showed strong redox signals of DA slightly higher than LHONA, which was clearly different from bare gold substrate (Figure S10, Supporting Information). The peak-to-peak separation ($E_{pa} - E_{pc}$) was 158 mV, which was slightly higher than that of chemical DA (58 mV), probably due to the cell membrane binding to the electrode that resulted in the increase of resistance. Next, to confirm the stability of electrochemical signals of DA released from PC12 cells, the signals from PC12 cells with or without L-DOPA pretreatment were compared based on the I_{pc} values of cyclic voltammogram with different cycle numbers. As shown in Figure 3e, the cathodic peaks from both groups were continuously appeared at around 0.21 and 0.04 μA

for L-DOPA pretreated and nontreated PC12 cells, respectively, with increasing cycle numbers up to 10. The cathodic peak from L-DOPA pretreated PC12 cells ($I_{pc} = 0.222$ μA) was ten times higher than L-DOPA nontreated PC12 cells ($I_{pc} = 0.022$ μA) at tenth cycle due to the increased amount of DA produced from cells via conversion of L-DOPA to DA, proving that the signals are highly stable and reliable which could be important for the determination of DA production capability of dopaminergic neurons (Figure S11, Supporting Information). The electrochemical signals achieved from PC12 cells were also found to increase as the increase of cell numbers, indicating that LHONA is reliable platform capable of detecting dopamine produced from cells in quantitative manner (Figure S12, Supporting Information). Finally, the DC amperometric method, a conventional tool that is useful for the simultaneous monitoring of changes in currents when applying a specific voltage,^[9] was further utilized to validate electrochemical DA signals of dopaminergic cells that were measured using CV. As expected, a clear spike-like currents appeared on the $i-t$ graph following addition of KCl (120×10^{-3} M) to trigger DA release while applying a cathodic voltage on PC12 cells, proving the presence of DA in PC12 cells which can be sensitively detected by LHONA substrate (Figure S13, Supporting Information).

Hence, it can be concluded that the fabricated large-scale homogeneous nanocup electrode arrays (LHONA) is a suitable material for the in situ monitoring of cellular signals, especially for the detection of DA from cells, mainly due to its outstanding electrochemical properties as well as its excellent biocompatibility.

Next, we attempted to detect DA signals from hNSC-derived dopaminergic neurons since the hNSC-derived dopaminergic neurons are the actual source of transplantation which could be utilized for the treatment of DA-related psychiatric diseases/disorders.^[4b,11] The hNSCs can be converted into dopamine-producing neurons through neurosphere generation, which are clusters of NSCs that still retain multipotency capable of differentiating into different types of neural cells. Since the dopaminergic neurons are only specific cell lines which express DDC that enables conversion of L-DOPA to DA, by detecting electrochemical signals of DA synthesized from L-DOPA, we can obtain some clues that prove the presence of DA-producing neurons derived from NSCs simply, easily, and precisely in completely noninvasive/nondestructive way.

To this end, hNSCs were differentiated into two different neurons—dopaminergic neuron and nondopaminergic neuron—and their electrochemical signals were compared with that of undifferentiated hNSCs, neurospheres, and premature neurons (Figure 4a). ReNcell VM cell line was chosen as a model stem cell line since it has been proven to be highly effective for the generation of dopaminergic neurons.^[12] Similar to the PC12 cells, dopaminergic neurons derived from hNSCs spread well on the surface of LHONA as shown in Figure S14 in the Supporting Information. To confirm the dopaminergic and nondopaminergic differentiation of hNSCs, respectively, cells were stained with tyrosine hydroxylase (TH), which is a representative marker of dopaminergic neurons.^[13] As shown in Figure 4b, only cells that have undergone dopaminergic differentiation showed TH expression while nondopaminergic cells failed to show any significant TH expression. A transcriptional activator for TH, Nurr 1, was also found to be highly expressed in the differentiated dopaminergic neurons when analyzed by real-time reverse transcription-PCR (Figure S15, Supporting Information). After the validation of dopaminergic differentiation of hNSCs, cells were detached and reseeded on the LHONA to confirm the difference between dopaminergic cells with other types of cells when analyzed by cyclic voltammetry. Remarkably, as hypothesized, only hNSC-derived dopaminergic neurons showed distinct redox peaks in voltammogram while its progenitor cells including hNSCs, neurospheres, and even premature neurons failed to show any reduction/oxidation peaks (Figure 4c, Figure S16 in the Supporting Information). I_{pc} value could only be calculated from dopaminergic neurons and was found to be approximately 0.13 μA , indicating that only dopaminergic neurons produced DA from externally added DA precursor (L-DOPA) via DDC (Figure 4d). To support these electrochemical results showing the ability of LHONA to detect dopamine and to distinguish dopaminergic neurons from other types of progenitor cells, the high-performance liquid chromatography (HPLC) was performed to confirm the dopamine release from L-DOPA pretreated dopaminergic neurons. We tested several different conditions: i) dopamine dissolved in medium, ii) medium collected from L-DOPA

pretreated hNSCs, iii) L-DOPA nontreated dopaminergic neurons derived from hNSCs, and iv) L-DOPA pretreated dopaminergic neurons. As shown in Figure S17 in the Supporting Information, only dopaminergic neurons pretreated with L-DOPA showed a clear dopamine peak (iv) while other groups failed to show the same peak, which were consistent with the electrochemical results.

Thereafter, to confirm that only functional dopaminergic neurons can produce DA from L-DOPA, cells were intentionally damaged by incubation with DPBS for different periods of time (30 min, 60 min, and 3 d) prior to the electrochemical detection. As shown in Figure S18 in the Supporting Information, the electrochemical signals were clearly detectable from the slightly damaged or nondamaged cells (30 min) while cells incubated with DPBS for longer period of time (60 min) showed decreased reduction peaks that were 28.6% lower than that of 30 min at the same reduction potential ($E_{pc} = -33$ mV). Finally, the voltammetric signals became completely negligible from the damaged dopaminergic neurons (cultured in DPBS for 3 d), proving that redox signals are only detectable from the viable/functional dopaminergic neurons, which will be highly useful to determine DA production ability of differentiated neurons prior to the clinical transplantation of them for replacing damaged/abnormal dopaminergic neurons that are responsible for many different types of neuronal diseases/disorders. Additionally, we also successfully confirmed that this distinct stable redox signals are not achievable from other type of similar neurons (nondopaminergic neurons), glial cells (astrocytes) and completely different cells (human dermal fibroblasts) with same conditions (L-DOPA pretreatment), indicating that redox peaks are only specific to functional dopaminergic neurons (Figure 4d and Figure S19, Supporting Information).

In conclusion, we have developed large-scale homogeneous nanocup electrode arrays (LHONA) for the effective detection of dopamine production from dopaminergic cell lines, as well as the monitoring of differentiation of hNSCs into dopaminergic neurons. LHONA bearing distinct cup-like nanostructures were successfully generated on transparent ITO electrode via two-step sequential process—LIL and ECD method. The LHONA platform showed excellent performance in the detection of chemical DA at both low range of concentrations ($0.3\text{--}3 \times 10^{-6}$ M, $R^2 = 0.99$) and high concentrations ($0\text{--}50 \times 10^{-6}$ M, $R^2 = 0.986$), with the LOD of 100×10^{-9} M, which was even higher than and other types of ITO-gold nanoparticle substrates, as well as the ITO modified with rGO. DA produced by model dopaminergic cells was found to be sensitively monitored on the LHONA due in part to its nanoscale pattern sizes and nanopotographical characteristics, which are large-scale periodic and homogeneous, that resulted in the enhancement of major functions of dopaminergic cells such as cell spreading, adhesion, and proliferations, as well as the enhanced sensitivity toward DA detection. Furthermore, due to the excellent biocompatibility and electrochemical performance of LHONA, the differentiation of hNSCs into dopaminergic neurons was successfully monitored, which showed distinct redox peaks that were clearly distinguished from its progenitor cells (e.g., hNSCs, neurospheres, and premature neurons), as well as the other cell types (e.g., nondopaminergic neurons, astrocytes, and fibroblasts). Since the destructive process such as cell lysis and fixation are totally excluded for detecting DA production and

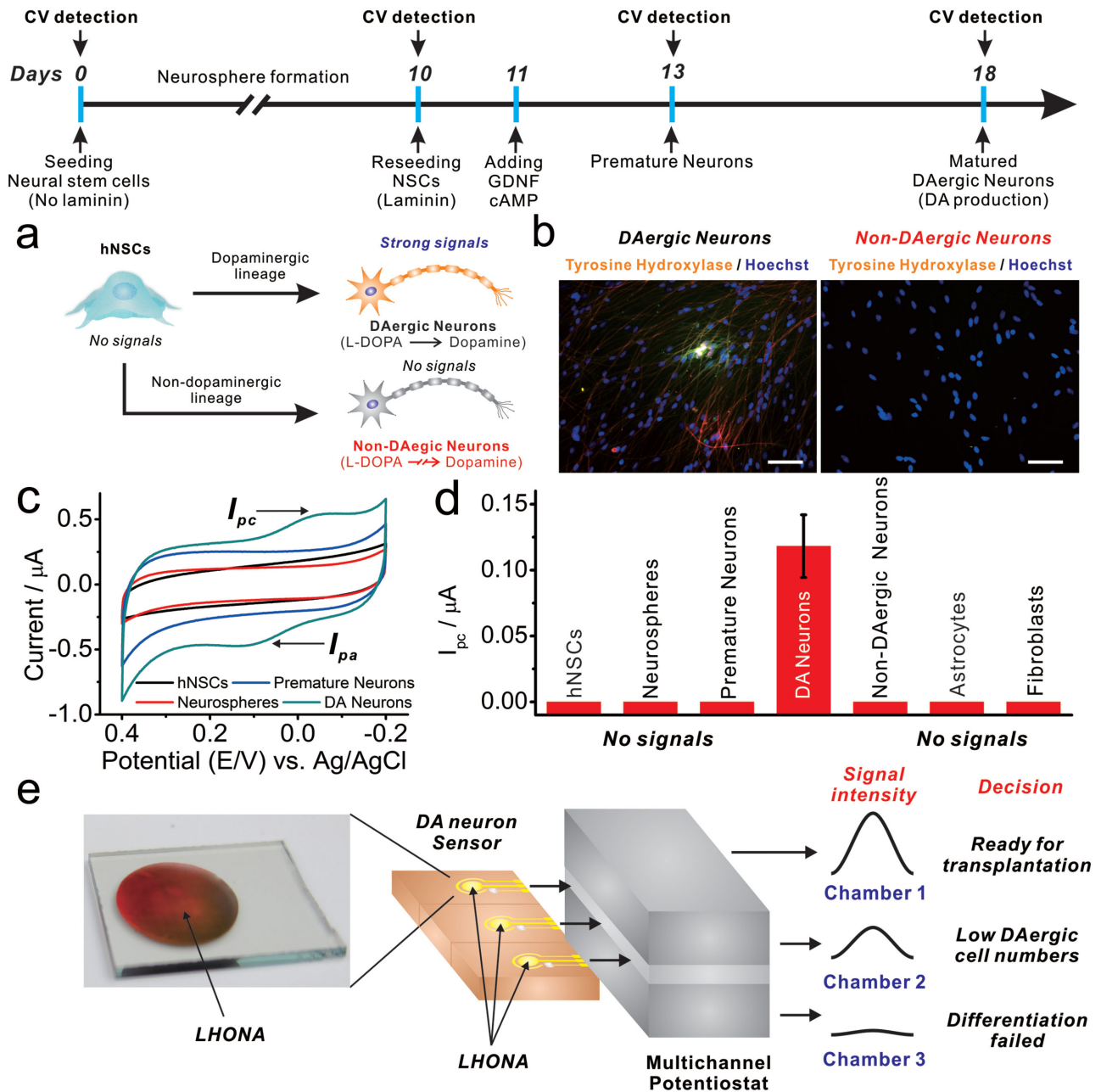


Figure 4. a) Schematic diagram showing the conversion of hNSCs into dopaminergic (DAergic) and non-DAergic neurons. b) Fluorescence images of cells stained with tyrosine hydroxylase to identify DAergic and non-DAergic neurons derived from hNSCs. Scale bar = 100 μm . c) Cyclic voltammogram achieved from cells undergoing differentiation into DAergic neurons (DA Neurons). Only completely matured DAergic neurons are showing distinct redox peaks as opposed to their progenitor cells (hNSCs, neurospheres, and premature neurons). d) I_{pc} values calculated from (c) and other types of cells (astrocytes and fibroblasts). "No signals" means that I_{pc} values cannot be calculated due to the absence of cathodic peaks. e) Possible strategy to use LHONA platform to confirm successful differentiation of NSCs into DAergic neurons and their DA production ability, which could be critical for making decision on the transplantation of DAergic neurons generated ex vivo.

monitoring dopaminergic differentiation of hNSCs, the developed periodic nanostructured platform (LHONA) and the electrochemical detection strategy introduced here can hold huge potential for preclinical testing of newly achieved dopaminergic neurons. Specifically, the LHONA platform can be useful for the assessment of the DA secretion from dopaminergic neurons derived from ESCs/iPSCs/NSCs/MSCs prior to the clinical

usage, as well as for the optimization of protocols to generate more dopaminergic neurons from pluripotent/multipotent stem cells in easy, simple but precise way (Figure 4e). Hence, it can be concluded that this work advances cell-based biosensors as an effective nondestructive in situ monitoring tool for stem-cell differentiation which can lead to more effective stem-cell-based therapies for incurable diseases/disorders.

Supporting Information

Supporting Information is available from the Wiley Online Library or from the author.

Acknowledgements

T.-H.K. and C.-H.Y. contributed equally to this work. J.-W.C. acknowledges financial support from Leading Foreign Research Institute Recruitment Program through the National Research Foundation of Korea (NRF) funded by the Ministry of Science, ICT & Future Planning (MSIP) (2013K1A4A3055268). K.-B.L. acknowledges financial support from the NIH R21 grant [1R21NS085569-01] and the N.J. Commission on Spinal Cord grant [CSR13ERG005].

Received: May 24, 2015

Revised: July 17, 2015

Published online: September 21, 2015

- [1] a) M. Guvendiren, J. A. Burdick, *Nat. Commun.* **2012**, *3*, 792; b) I. L. Weissman, *Science* **2000**, *287*, 1442; c) A. M. Maroof, S. Keros, J. A. Tyson, S. W. Ying, Y. M. Ganat, F. T. Merkle, B. Liu, A. Goulburn, E. G. Stanley, A. G. Elefanty, H. R. Widmer, K. Eggan, P. A. Goldstein, S. A. Anderson, L. Studer, *Cell Stem Cell* **2013**, *12*, 559; d) T.-H. Kim, S. Shah, L. Yang, P. T. Yin, M. K. Hossain, B. Conley, J.-W. Choi, K.-B. Lee, *ACS Nano* **2015**, *9*, 3780; e) F. Guilak, D. M. Cohen, B. T. Estes, J. M. Gimble, W. Liedtke, C. S. Chen, *Cell Stem Cell* **2009**, *5*, 17; f) A. J. Engler, S. Sen, H. L. Sweeney, D. E. Discher, *Cell* **2006**, *126*, 677; g) V. Castiglioni, M. Onorati, C. Rochon, E. Cattaneo, *Neurobiol. Dis.* **2012**, *46*, 30; h) P. T. Yin, S. Shah, M. Chhowalla, K.-B. Lee, *Chem. Rev.* **2015**, *115*, 2483.
- [2] a) S. Shah, P. T. Yin, T. M. Uehara, S. T. D. Chueng, L. T. Yang, K. B. Lee, *Adv. Mater.* **2014**, *26*, 3673; b) M. Nikkha, F. Edalat, S. Manoucheri, A. Khademhosseini, *Biomaterials* **2012**, *33*, 5230; c) D. W. Han, N. Tapia, A. Hermann, K. Hemmer, S. Hoing, M. J. Arauzo-Bravo, H. Zaehres, G. M. Wu, S. Frank, S. Moritz, B. Greber, J. H. Yang, H. T. Lee, J. C. Schwamborn, A. Storch, H. R. Scholer, *Cell Stem Cell* **2012**, *10*, 465; d) M. Bellin, M. C. Marchetto, F. H. Gage, C. L. Mummery, *Nat. Rev. Mol. Cell Biol.* **2012**, *13*, 713.
- [3] L. Qiang, R. Fujita, A. Abeliovich, *Neuron* **2013**, *78*, 957.
- [4] a) M. Wernig, J. P. Zhao, J. Pruszak, E. Hedlund, D. D. Fu, F. Soldner, V. Broccoli, M. Constantine-Paton, O. Isacson, R. Jaenisch, *Proc. Natl. Acad. Sci. USA* **2008**, *105*, 5856; b) O. Lindvall, Z. Kokaia, A. Martinez-Serrano, *Nat. Med.* **2004**, *10*, S42; c) J. H. Kim, J. M. Auerbach, J. A. Rodriguez-Gomez, I. Velasco, D. Gavin, N. Lumelsky, S. H. Lee, J. Nguyen, R. Sanchez-Pernaute, K. Bankiewicz, R. McKay, *Nature* **2002**, *418*, 50.
- [5] a) M. J. P. Biggs, R. G. Richards, N. Gadegaard, C. D. W. Wilkinson, R. O. C. Oreffo, M. J. Dalby, *Biomaterials* **2009**, *30*, 5094; b) K. R. Milner, C. A. Siedlecki, *J. Biomed. Mater. Res., Part A* **2007**, *82*, 80; c) R. J. McMurray, N. Gadegaard, P. M. Tsimbouri, K. V. Burgess, L. E. McNamara, R. Tare, K. Murawski, E. Kingham, R. O. C. Oreffo, M. J. Dalby, *Nat. Mater.* **2011**, *10*, 637; d) K. Kulangara, Y. Yang, J. Yang, K. W. Leong, *Biomaterials* **2012**, *33*, 4998; e) D. H. Kim, P. P. Provenzano, C. L. Smith, A. Levchenko, *J. Cell Biol.* **2012**, *197*, 351; f) M. J. Dalby, N. Gadegaard, R. O. C. Oreffo, *Nat. Mater.* **2014**, *13*, 558; g) W. Q. Chen, L. G. Villa-Diaz, Y. B. Sun, S. N. Weng, J. K. Kim, R. H. W. Lam, L. Han, R. Fan, P. H. Krebsbach, J. P. Fu, *ACS Nano* **2012**, *6*, 4094.
- [6] a) H. F. Cui, J. S. Ye, Y. Chen, S. C. Chong, X. Liu, T. M. Lim, F. S. Sheu, *Sens. Actuators, B* **2006**, *115*, 634; b) L. Amato, A. Heiskanen, C. Caviglia, F. Shah, K. Zor, M. Skolimowski, M. Madou, L. Gammelgaard, R. Hansen, E. G. Seiz, M. Ramos, T. R. Moreno, A. Martinez-Serrano, S. S. Keller, J. Emneus, *Adv. Funct. Mater.* **2014**, *24*, 7042.
- [7] M. B. Hariri, A. Dolati, R. S. Moakhar, *J. Electrochem. Soc.* **2013**, *160*, D279.
- [8] a) M. Zhou, Y. M. Zhai, S. J. Dong, *Anal. Chem.* **2009**, *81*, 5603; b) L. H. Tang, Y. Wang, Y. M. Li, H. B. Feng, J. Lu, J. H. Li, *Adv. Funct. Mater.* **2009**, *19*, 2782; c) S. Alwarappan, A. Erdem, C. Liu, C. Z. Li, *J. Phys. Chem. C* **2009**, *113*, 8853.
- [9] H. F. Cui, J. S. Ye, Y. Chen, S. C. Chong, F. S. Sheu, *Anal. Chem.* **2006**, *78*, 6347.
- [10] M. A. Kafi, W. A. El-Said, T. H. Kim, J. W. Choi, *Biomaterials* **2012**, *33*, 731.
- [11] G. H. Petit, T. T. Olsson, P. Brundin, *Neuropathol. Appl. Neurobiol.* **2014**, *40*, 60.
- [12] a) S. Pai, F. Verrier, H. Y. Sun, H. B. Hu, A. M. Ferrie, A. Eshraghi, Y. Fang, *J. Biomol. Screening* **2012**, *17*, 1180; b) R. Donato, E. A. Miljan, S. J. Hines, S. Aouabdi, K. Pollock, S. Patel, F. A. Edwards, J. D. Sinden, *BMC Neurosci.* **2007**, *8*, 36; c) Z. L. Chaudhry, B. Y. Ahmed, *Neurol. Res.* **2013**, *35*, 435.
- [13] M. Caiazzo, M. T. Dell'Anno, E. Dvoretzkova, D. Lazarevic, S. Taverna, D. Leo, T. D. Sotnikova, A. Menegon, P. Roncaglia, G. Colciago, G. Russo, P. Carninci, G. Pezzoli, R. R. Gainetdinov, S. Gustincich, A. Dityatev, V. Broccoli, *Nature* **2011**, *476*, 224.